Regional Lumped Constant Differences and Asymmetry in Fluorine-18-FDG Uptake in Temporal Lobe Epilepsy

David C. Reutens, Albert H. Gjedde and Ernst Meyer

Positron Imaging Laboratories; McConnell Brain Imaging Centre; Montreal Neurological Institute; and McGill University, Montreal, Canada

To date, there has been no satisfactory explanation for the observation that interictal uptake of the glucose analog [^{18}F]fluorodeoxyglucose (FDG) is consistently reduced in the temporal lobe ipsilateral to the seizure focus in patients with temporal lobe epilepsy. We examined the hypothesis that regional differences in tracer uptake in temporal lobe epilepsy reflect regional differences in the lumped constant (Λ). **Methods:** In 9 control subjects and 10 patients with temporal lobe epilepsy, we obtained regional estimates of Λ by expressing Λ in terms of transfer coefficients for FDG and parameters which are likely to remain constant throughout both the brain and under different functional states. **Results:** In the patients, Λ was lower in the temporal lobe ipsilateral to the epileptic focus (0.53 ± 0.06; $p < 0.005$) than in the contralateral temporal lobe (0.56 ± 0.06). Interside differences in Λ were highly correlated with asymmetry in tracer uptake. Furthermore, the use of regional estimates of Λ reduced the asymmetry in estimated $rCMR_{glc}$ in patients with temporal lobe epilepsy but not in controls. **Conclusion:** In these patients, a change in tracer uptake may not indicate a change in glucose consumption of corresponding magnitude, raising the possibility that in at least some patients with temporal lobe epilepsy, the term hypometabolism does not accurately describe reductions in tracer uptake.

Key Words: fluorine-18-fluorodeoxyglucose, PET, temporal lobe epilepsy

J Nucl Med 1998; 39:176–180

In temporal lobe epilepsy, reduced uptake of the glucose analog [^{18}F]fluorodeoxyglucose (FDG) is consistently found in the temporal lobe ipsilateral to the epileptic focus during the interictal period (*1–4*). Relative reductions in tracer uptake appear to be greater in the lateral than in the mesial temporal cortex (*1,3,4*). These reductions in tracer uptake are frequently equated with hypometabolism of glucose, and several theories have been advanced to explain such a change in metabolic state. It has been suggested that localized neuronal loss contributes to hypometabolism (*5*). However, severe reductions in tracer uptake may occur even in the absence of quantified neuronal loss or gliosis in the temporal neocortex (*6*). A second hypothesis is that diaschisis associated with hippocampal neuronal loss produces interictal hypometabolism. The poor correlation between changes in FDG uptake in the temporal neocortex and hippocampal cell counts goes against this hypothesis (*7*). Further, contrary evidence is provided by the tendency for neocortical tracer uptake to normalize after selective amygdalohippocampectomy (*8*).

An alternative explanation for changes in tracer uptake may lie in the FDG methodology itself. FDG competes with glucose for carrier-mediated transport into the brain and serves as an alternative substrate for hexokinase. To estimate the rate of glucose consumption, a proportionality factor termed the lumped constant (Λ), is applied to the rate of phosphorylation of FDG. In general, Λ is assumed to be invariant throughout the brain, and while this assumption is approximately true under normal conditions, pathological states may produce regional differences in the lumped constant (*9*). By expressing Λ in terms of transfer coefficients for FDG and parameters, which are likely to remain constant both throughout the brain and under different functional states, we examined the issue of the constancy of Λ in patients with temporal lobe epilepsy.

MATERIALS AND METHODS

Subjects

We studied 9 neurologically normal subjects (2 men, 7 women; mean age 24 yr) and 10 subjects (3 men, 7 women; mean age 31 yr) with intractable temporal lobe epilepsy. All patients had unilateral mesial temporal epilepsy as judged from video-EEG monitoring of seizures, unilateral hippocampal atrophy on MRI and the response to resection in eight patients. Interictal PET scans were performed with the patients being free of clinical seizures for at least 24 hr before PET scanning. Subjects fasted overnight before the scan.

PET Scanning

Dynamic FDG-PET studies were performed with a Scanditronix PC-2048 15B scanner which produces 15 slices with an intrinsic resolution of 6 mm × 6 mm × 6 mm. A foam head mould was fitted to minimize head movement. Subjects were positioned in the scanner so that the PET slices were parallel to the orbitomeatal line and both temporal lobes were entirely contained in the field of view. A ^{68}Ge orbiting rod transmission source was used for attenuation correction.

After the intravenous injection of a slow bolus of FDG (5 mCi over ~1 min), brain radioactivity was measured over a period of 30 min using a scan schedule of six 30-sec scans, seven 1-min scans, five 2-min scans and two 5-min scans. Plasma radioactivity was measured in arterial blood sampled every 10 sec from 0–3 min; every 20 sec from 3–5 min; and every 1–5 min until 30 min after the injection of FDG. Arterial plasma glucose concentrations were measured at 10-min intervals throughout the study.

All subjects underwent MRI (Philips Gyroscan 1.5T) with scans consisting of 160 contiguous slices of 1 mm thickness and 1 mm by 1 mm pixel dimension.

Image Analysis

To obtain maps of unidirectional blood-brain clearance (K_1^*) and the net uptake constant (K^*), PET images were reconstructed using an 18-mm FWHM Hanning filter, and individual

Received Nov. 4, 1996; revision accepted Apr. 14, 1997.

For correspondence or reprints contact: David C. Reutens, MD, Montreal Neurological Institute, 3801 University St., Montreal, Quebec, Canada H3A 2B4.

TABLE 1
Kinetic Parameters in the Temporal Lobes Ipsilateral and Contralateral to the Seizure Focus and in the Temporal Lobes of Control Subjects*

	Epilepsy		Control	
	Ipsilateral	Contralateral	Right	Left
K^* (μl/g/min)	27.7 ± 11.3†	29.9 ± 12.2	29.6 ± 10.8	29.7 ± 11.5
K_1^* (μl/g/min)	90.8 ± 24.4	88.4 ± 24.4	87.5 ± 17.9	88.4 ± 18.9
Lumped constant rCMRglc	0.53 ± 0.06†	0.56 ± 0.06	0.55 ± 0.06	0.55 ± 0.06
$\Lambda = 0.56$	24.6 ± 9.9†	26.6 ± 10.8	27.1 ± 9.0	27.2 ± 9.6
Regional Λ	25.2 ± 8.6‡	26.0 ± 8.9	26.8 ± 7.5	26.9 ± 8.0
Asymmetry in rCMRglc (%)				
$\Lambda = 0.56$	7.2 ± 4.3		−0.3 ± 6.0	
Regional Λ	3.1 ± 2.5		0.0 ± 4.5	

*Plasma clearance (K_1^*), the net uptake constant (K), the lumped constant (Λ), the rate of glucose consumption (rCMRglc) and asymmetry indices for rCMRglc estimated using a fixed Λ and regional estimates of Λ are compared (mean ± s.d.).
†$p < 0.005$.
‡$p < 0.01$.

time-activity curves for each voxel were fitted with a three-compartment model using a previously described method of analysis (*10*). Voxel-based maps of Λ were then generated using a transport ratio of 1.1 and a phosphorylation ratio of 0.3 (see Appendix). Images of radioactivity, summed overall frames of the PET scan were also generated.

PET and MRI images were co-registered (*11*) and MRI-based regions of interest (ROIs) were drawn, using predetermined anatomical landmarks for guidance, over each temporal lobe. For voxels within these regions, mean values were calculated for Λ, for summed radioactivity and for K_1^* and K^*. For each patient, the regional metabolic rate for glucose ($rCMR_{glc}$) was calculated using the mean plasma glucose concentration during the PET scan, the mean value for K^* in each ROI and [i] $\Lambda = 0.56$ or [ii] the mean calculated value of Λ for each ROI. An asymmetry index for $rCMR_{glc}$ estimated using fixed or regional Λ values was then calculated:

$$\text{Asymmetry index (\%)} = 100 \times \frac{\text{Contralateral } rCMR_{glc} - \text{Ipsilateral } rCMR_{glc}}{\text{Contralateral } rCMR_{glc}}. \quad \text{Eq. 1}$$

To ensure that the results obtained were independent of the method of data analysis, kinetic parameters were also estimated using time-activity curves in smaller ROIs drawn over each temporal lobe. In this analysis, PET images were reconstructed using an 6-mm FWHM Hanning filter. Nonlinear least squares fitting was used with the operational equation described in the Appendix.

Statistical Analysis

The statistical significance of interside differences in parameter values was assessed using the paired Student's t-test. The unpaired Student's t-test was used to compare parameters from patients and controls. The correlation between asymmetry indices for summed radioactivity and Λ was assessed using Pearson's correlation coefficient (r).

RESULTS

Analysis of Parametric Images

The mean plasma glucose concentration was similar in patients (5.0 ± 0.5 m*M*, mean ± s.d.) and in control subjects (5.2 ± 0.6 m*M*). In control subjects, the mean sizes of the volumes of interest were 74.4 ± 13.9 cm^3 and 75.4 ± 10.3 cm^3 for the right and left temporal lobes, respectively. In patients with epilepsy, the mean sizes were 70.2 ± 14.3 cm^3 in the temporal lobe ipsilateral to the seizure focus and 75.1 ± 11.6 cm^3 in the contralateral temporal lobe. The mean value of the net uptake constant (K^*) was significantly lower ipsilateral to the seizure focus (Table 1). The mean value of K_1^* did not differ significantly between temporal lobes.

Lumped Constant

In control subjects, there was no significant difference between the mean values of Λ for the right and left temporal lobes (0.55 ± 0.06). In contrast, the mean value of Λ was significantly lower in the temporal lobe ipsilateral to the epileptic focus (0.53 ± 0.06) than in the contralateral temporal lobe (0.56 ± 0.06; $p < 0.005$; Table 1; Fig. 1).

Correlation Between Asymmetry in Radioactivity and the Lumped Constant

The mean asymmetry index in summed radioactivity was −1.1% ± 2.5% in control subjects and 3.9% ± 3.9% ($p < 0.05$) in patients with epilepsy. None of the control subjects had an asymmetry index greater than 4% whereas this was present in 6 of 10 patients ($p < 0.05$; Fisher exact test). Asymmetry in Λ

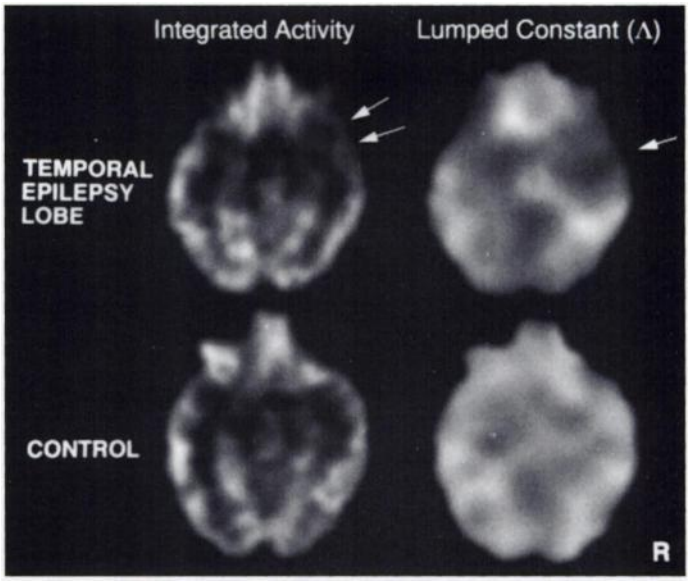

FIGURE 1. Images of tracer uptake (integrated activity) and the estimated lumped constant in a control subject and a patient with temporal lobe epilepsy. In the patient with temporal lobe epilepsy, reduced tracer uptake is observed in the right temporal lobe (↑ ↑). In the lumped constant image a corresponding reduction in the estimated lumped constant is observed (↑).

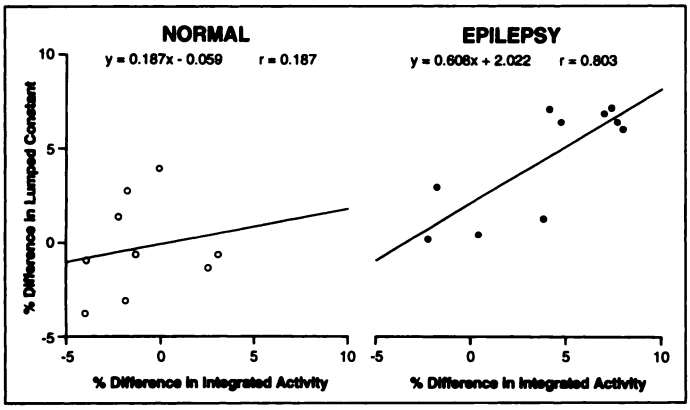

FIGURE 2. Correlation between regional asymmetry in estimated lumped constant and asymmetry in tracer uptake (integrated radioactivity). Asymmetry between right and left temporal lobes in normal subjects and between the temporal lobes ipsilateral and contralateral to the seizure focus in patients with temporal lobe epilepsy are shown.

correlated significantly with asymmetry in summed activity in patients with epilepsy ($r = 0.8$; $p < 0.01$) but not in control subjects ($r = 0.19$; $p = 0.63$; Fig. 2).

Influence of Lumped Constant Estimates on $rCMR_{glc}$

With a fixed Λ of 0.56, the mean $rCMR_{glc}$ was significantly lower in the temporal lobe ipsilateral to the epileptic focus than in the contralateral temporal lobe (24.6 ± 9.9 versus 26.6 ± 10.8 μmol 100 g^{-1} min^{-1}, respectively; $p < 0.005$). The use of regional estimates of Λ reduced the interside difference in $rCMR_{glc}$ (Table1). In control subjects, the mean $rCMR_{glc}$ in the right and left temporal lobes was not significantly different.

Compared to fixing Λ, regional estimation of Λ significantly reduced the degree of asymmetry in $rCMR_{glc}$ between ipsilateral and contralateral temporal lobes in patients with epilepsy (3.1% versus 7.2%; $p < 0.005$; Table 1). In contrast, no significant change in the degree of asymmetry was observed in control subjects. With a fixed Λ, the degree of asymmetry was significantly greater in patients than in controls (7.2% versus −0.3%; $p < 0.01$), but with regional estimates of Λ, there was no significant difference between the two groups in the degree of asymmetry (3.1% versus 0.0%; $p = 0.1$).

The use of regional estimates of Λ had a greater effect on asymmetry in $rCMR_{glc}$ in the six patients with more than 4% asymmetry in summed radioactivity. In these patients, mean asymmetry in $rCMR_{glc}$ was 3.4% ± 2.9% when regional estimates of Λ were used. In contrast, it was 10.0% ± 3.0% when Λ was fixed.

Nonlinear Least Squares Fitting

For this analysis, we used an average of seven ROIs within each temporal lobe with mean sizes of 1.2 ± 0.4 cm^3 ipsilateral and 1.3 ± 0.3 cm^3 contralateral to the seizure focus in patients and 1.3 ± 0.4 cm^3 and 1.3 ± 0.5 cm^3 in the right and left temporal lobes of control subjects. In control subjects, there was no significant difference between the mean values of Λ for the right (0.56 ± 0.10) and left (0.55 ± 0.08) temporal lobes. The mean value of Λ was significantly lower in the temporal lobe ipsilateral to the epileptic focus (0.52 ± 0.06) than in the contralateral temporal lobe (0.58 ± 0.07; $p < 0.05$).

DISCUSSION

The principal findings of this study are threefold. First, in patients with temporal lobe epilepsy, Λ was lower in the temporal lobe ipsilateral to the epileptic focus than in the contralateral temporal lobe. Second, interside differences in Λ were highly correlated with asymmetry in tracer uptake. Third, the use of regional estimates of Λ reduced the asymmetry in estimated $rCMR_{glc}$ in patients with temporal lobe epilepsy but not in controls.

Lumped Constant Variability (Λ)

In this study, asymmetry of Λ in patients with temporal lobe epilepsy was detected using voxel-based estimates of K^* and K_1^* obtained with a solution of the model differential equations that allowed the use of linear regression. Asymmetry of Λ was also detected using a ROI-based analysis, nonlinear least squares fitting and less smoothing of the PET image.

The lumped constant is a key aspect of the use of FDG to estimate cerebral glucose consumption. It is a proportionality factor that converts the rate of phosphorylation of FDG to the net rate of glucose consumption. As originally proposed by Sokoloff et al. (*12*), Λ is the product of four factors: the fraction of glucose that continues down the glycolytic pathway and the hexose monophosphate shunt after phosphorylation; the ratio between the steady state volume of distribution of FDG and of glucose; the ratio between the maximum velocities of phosphorylation of FDG and of glucose by hexokinase; and the ratios between the Michaelis-Menten constants of hexokinase for FDG and for glucose. Sokoloff et al. (*12*) provided theoretical grounds for the constancy of some of these factors and proposed that Λ was uniform throughout the brain. However, the ratio between the steady-state volumes of distribution of tracer and of glucose, each being differently influenced by blood flow, blood-brain barrier transport and metabolism, is a potential source of state-dependent variation in Λ (*13*).

Subsequent formulations have expressed Λ in terms of kinetic parameters for the uptake of FDG and factors which are more likely to be constant than Λ or the steady-state distribution volume ratio thus allowing Λ to be estimated locally (see Appendix) (*14,15*). Our estimates of Λ are close to previously reported values in humans [0.5, Brooks et al. (*16*); 0.52, Reivich et al. (*17*)].

Estimates of Λ were significantly lower in the temporal lobe ipsilateral to the seizure focus than in the contralateral temporal lobe. This reflects a change in the balance between the blood-brain barrier transport and the phosphorylation of FDG and glucose in the epileptic temporal lobe. In the normal brain, glucose transport and metabolism appear to be closely linked (*18–20*). However, in the temporal lobe ipsilateral to the seizure focus, a reduction in the mean value of the net uptake constant (K^*) was observed whereas there was no significant change in K_1^*, the unidirectional plasma clearance of FDG. The observation that changes in K^* are not parallelled by changes in K_1^* in the epileptic temporal lobe requires explanation. In the epileptic temporal lobe, K_1^* reflects changes, most likely in opposing directions, in blood flow and in the permeability of the blood-brain barrier to glucose and FDG. Sustained changes in the density of the glucose transporter may occur in response to seizures. In tissue from a patient undergoing surgery for epilepsy, Cornford et al. (*21*) observed a higher density of the Glut 1 glucose transporter in the blood-brain barrier than previously described in the capillaries of rat and rabbit brains. Increased expression of the glucose transporter gene is also seen in other states, such as ischemia, where glucose demand outstrips supply (*22*). Indeed, such a mechanism may be an adaptive response protecting against seizure-induced neuron loss (*23*). In addition, there may be a mismatch between changes in blood flow and in glucose consumption in the epileptic temporal lobe; unlike K^*, K_1^* is strongly affected by blood flow.

Stability of the Phosphorylation and Transport Ratios

The estimates of Λ obtained in this study are dependent on the values chosen for the phosphorylation and transport ratios. The validity of the chosen values for these ratios was discussed previously in Kuwabara et al. (*24*). Inspection of the equation for Λ (see Appendix, Eq. 7) reveals that because the ratio between K^* and K_1^* is regionally variant in our patients, Λ can only be truly constant if the phosphorylation ratio and the transport ratio are equal. However, there is considerable evidence that this is not the case (*25–29*). FDG is transported across the blood-brain barrier at a greater rate but is phosphorylated at a lower rate than glucose.

There are strong theoretical reasons for assuming that the transport and phosphorylation ratios are constant across brain regions and metabolic states (*12,14,24*). However, regional changes in the phosphorylation ratio due to expression of isoenzymes of hexokinase normally found in muscle and liver have been described in brain tumors (*9*). Such a process is unlikely in epileptic tissue and is amenable to in vitro verification.

Implications for FDG-PET Scans in Epilepsy

Compared to fixing Λ, the use of regional estimates of Λ resulted in a reduction in the asymmetry of $rCMR_{glc}$ in the patients. However, $rCMR_{glc}$ remained significantly lower ipsilateral to the seizure focus than contralaterally when regional estimates of Λ were used.

The finding of a consistent reduction in Λ in the temporal lobe ipsilateral to the seizure focus resolves several apparent inconsistencies. This mechanism allows for reductions in the uptake of FDG which are not linked to cell loss, in keeping with the previously observed poor correlation between tracer uptake and neuronal density in the hippocampus and temporal neocortex (*7*). In addition, reversible changes in Λ may contribute to the normalization of tracer uptake after seizure cessation induced by selective amygdalo-hippocampectomy (*8*). Furthermore, regional variations in Λ may explain previous findings of discordance between asymmetry in $rCMR_{glc}$ and regional cerebral blood flow in temporal lobe epilepsy (*30,31*). When a fixed Λ is used, the relative reduction in $rCMR_{glc}$ exceeds that for regional cerebral blood flow in the epileptic temporal lobe (*32,33*).

Our findings indicate that the use of a single value of Λ for the whole brain leads to errors in $rCMR_{glc}$ determination in patients with temporal lobe epilepsy and exaggerates the observed degree of asymmetry in $rCMR_{glc}$. To the extent that the diagnostic use of nonquantitative scans depends only on the correlation between seizure focus lateralization and asymmetry in tracer uptake, regardless of the underlying mechanism, our findings should not affect the practical utilization of FDG-PET in temporal lobe epilepsy. However, the findings indicate that a change in tracer uptake does not necessarily signify a change in glucose consumption of corresponding magnitude.

CONCLUSION

We conclude that Λ is lower in the temporal lobe ipsilateral to the epileptic focus than in the contralateral temporal lobe in patients with temporal lobe epilepsy. The use of regional estimates of Λ reduces asymmetry in estimated $rCMR_{glc}$ in patients with temporal lobe epilepsy but not in controls. Changes in Λ should be considered when ascribing a biological interpretation to changes in tracer uptake. Indeed, in at least some patients with temporal lobe epilepsy, the term hypometabolism may not accurately describe reductions in tracer uptake.

APPENDIX

The net uptake constant (K^*) for FDG is defined as:

$$K^* = \frac{K_1^* k_3^*}{k_2^* + k_3^*}, \qquad \text{Eq. 2}$$

where K_1^* refers to the unidirectional plasma clearance, k_2^* to the fractional brain-blood clearance and k_3^* is the phosphorylation coefficient (*34*). Symbols relating to FDG are denoted with an asterisk. The glucose metabolic rate ($rCMR_{glc}$) is expressed in terms of K^*, glucose concentration (C_a) and the lumped constant (Λ):

$$rCMR_{glc} = \frac{K^* C_a}{\Lambda}. \qquad \text{Eq. 3}$$

The processes of facilitated diffusion of hexoses across the blood-brain barrier and of phosphorylation by hexokinase can be described by the Michaelis-Menten equation (*24*). In the case of transport across the blood-brain barrier, the Michaelis-Menten equation yields an approximately constant ratio (τ, the transport ratio) between FDG and glucose clearances:

$$\tau = \frac{K_t K_{max}^*}{K_t^* T_{max}} = \frac{P^* S^*}{PS} \cong \frac{K_1^*}{K_1}, \qquad \text{Eq. 4}$$

where PS is the apparent permeability-surface area product for the blood-brain barrier, K_t is the half-saturation constant, and T_{max} is the maximal transport rate.

Similarly, the ratio between the rate constants for the phosphorylation of FDG and of glucose by hexokinase (φ, the phosphorylation ratio) can be expressed in terms of the Michaelis-Menten equation:

$$\varphi = \frac{K_m V_{max}^*}{K_m^* V_{max}} = \frac{k_3^*}{k_3}, \qquad \text{Eq. 5}$$

where K_m is the half-saturation constant, and V_{max} is the maximal velocity of phosphorylation by hexokinase.

The phosphorylation ratio and the transport ratio are likely to remain constant both throughout the brain and in different functional states. While the maximum velocities of transport and of phosphorylation of FDG and glucose are likely to vary according to the regional variation in transporter protein and hexokinase concentrations, respectively, the maximum velocities for FDG and for glucose are likely to vary proportionally (*12*). Thus, T^*/T_{max} and V_{max}^*/V_{max} are likely to remain constant. K_t and K_m represent kinetic properties of the hexose transporter protein and of hexokinase, respectively, and can also be expected to remain constant throughout the brain (*12*).

The lumped constant for FDG (Λ) can be expressed as:

$$\Lambda = \frac{K^*}{K} = \frac{K^*(k_2 + k_3\Phi)}{K_1 k_3 \Phi}, \qquad \text{Eq. 6}$$

where Φ is the fraction of glucose-6-phosphate further metabolized (*24*). By assuming that the partition volume ($V_e = K_1/k_2 = K_1^*/k_2^*$) is the same for glucose and its analogs (*35*), expressing K_1 in terms of K_1^* and the transport ratio (τ) and expressing k_3 in terms of k_3^* and the phosphorylation ratio (φ), Equation 6 simplifies to:

$$\Lambda = \frac{\varphi}{\Phi} + \left(\tau - \frac{\varphi}{\Phi}\right)\frac{K^*}{K_1^*}. \qquad \text{Eq. 7}$$

Using this formulation, changes in Λ can be identified if there is a change in the ratio between K^* and K_1^*. In this study, regional estimates of Λ were obtained using Equation 7, estimates of K_1^* and K^* and published values of φ and τ (*24*). Because the activity of glucose-6-phosphatase is low, we assumed that Φ = 1.

Generation of maps of K_1^* and K^* was accomplished with the following operational equation:

$$M_T^*(T) = K_1^* k_3^* \int_0^T \int_0^u C_a^*(t)\, dt du + [K_1^* + V_0(k_2^* + k_3^*)] \int_0^T C_a^*(t)\, dt + V_0 C_a^*(T) - (k_2^* + k_3^*) \int_0^T M_T^*(t)\, dt, \quad \text{Eq. 8}$$

where M_T^* refers to measured tissue radioactivity, C_a^* is arterial tracer concentration and V_0 is a term which corrects for tracer activity in brain vascular volume. In the region of interest-based analysis, nonlinear least squares fitting was used to estimate kinetic parameters using the following operational equation:

$$M_T^*(T) = K^* \int_0^T C_a(t)\, dt + (K_1^* - K^*) \int_o^T e^{(k_2^* + k_3^*)(t-T)} C_a(t)\, dt + V_0 C_a(T). \quad \text{Eq. 9}$$

ACKNOWLEDGMENTS

Dr. Reutens was supported by a Neil Hamilton Fairley Fellowship of the National Health and Medical Research Council of Australia. Dr. Meyer was supported by the Isaac Walton Killam Fellowship Fund of the Montreal Neurological Institute. We thank the technical and cyclotron staff of the McConnell Brain Imaging Center for their untiring efforts and Drs. F. Andermann and F. Dubeau for allowing us to study their patients. The project was supported by MRC grant SP-30 (Canada).

REFERENCES

1. Sackellares JC, Siegel GJ, Abou-Khalil BW, et al. Differences between lateral and mesial temporal metabolism interictally in epilepsy of mesial temporal origin. *Neurology* 1990;40:1420–1426.
2. Engel J, Kuhl DE, Phelps ME, Mazziotta JC. Interictal cerebral glucose metabolism in partial epilepsy and its relation to EEG changes. *Ann Neurol* 1982;12:510–517.
3. Henry TR, Mazziotta JC, Engel J, et al. Quantifying interictal metabolic activity in human temporal lobe epilepsy. *J Cereb Blood Flow Metab* 1990;10:748–757.
4. Abou-Khalil B, Siegel GJ, Hichwa RD, Sackellares JC, Gilman S. Topography of glucose hypometabolism in epilepsy of mesial temporal origin. *Ann Neurol* 1985;18: 151–152.
5. Engel J, Brown WJ, Kuhl DE, Phelps ME, Mazziotta JC, Crandall PH. Pathological findings underlying focal temporal lobe hypometabolism in partial epilepsy. *Ann Neurol* 1982;12:518–528.
6. Henry TR, Mazziotta JC, Engel J. Interictal metabolic anatomy of mesial temporal lobe epilepsy. *Arch Neurol* 1993;50:582–589.
7. Henry TR, Babb TL, Engel J, Mazziotta JC, Phelps ME, Crandall PH. Hippocampal neuronal loss and regional hypometabolism in temporal lobe epilepsy. *Ann Neurol* 1994;36:925–927.
8. Hajek M, Wieser HG, Khan N, et al. Preoperative and postoperative glucose consumption in mesiobasal and lateral temporal lobe epilepsy. *Neurology* 1994;44: 2125–2132.
9. Kapoor R, Spence AM, Muzi M, Graham MM, Abbott GL, Krohn KA. Determination of the deoxyglucose and glucose phosphorylation ratio and the lumped constant in rat brain and a transplantable rat glioma. *J Neurochem* 1989;53:37–44.
10. Blomqvist G. On the construction of functional maps in positron emission tomography. *J Cereb Blood Flow Metab* 1984;4:629–632.
11. Woods RP, Mazziotta JC, Cherry SC. MRI-PET registration with automated algorithm. *J Comput Assist Tomogr* 1993;17:536–546.
12. Sokoloff L, Reivich M, Kennedy C, et al. The [^{14}C]deoxyglucose method for the measurement of local cerebral glucose utilization: theory, procedure, and normal values in the conscious and anesthetized albino rat. *J Neurochem* 1977;28:897–916.
13. Mori K, Cruz N, Dienel G, Nelson T, Sokoloff L. Direct chemical measurement of the λ of the lumped constant of the [^{14}C]deoxyglucose method in rat brain: effects of arterial plasma glucose level on the distribution spaces of [^{14}C]deoxyglucose and glucose and on λ. *J Cereb Blood Flow Metab* 1989;9:304–314.
14. Holden JE, Mori K, Dienel GA, Cruz NF, Nelson T, Sokoloff L. Modeling the dependence of hexose distribution volumes in brain on plasma glucose concentration: implications for estimation of the local 2-deoxyglucose lumped constant. *J Cereb Blood Flow Metab* 1991;11:181–182.
15. Phelps ME, Huang S-C, Mazziotta JC, Hawkins RA. Alternate approach for examining stability of the deoxyglucose model lumped constant. *J Cereb Blood Flow Metab* 1983;3(suppl 1):S13–S14.
16. Brooks RA, Hatazawa J, Di Chiro G, Larson SM, Fishbein DS. Human cerebral glucose metabolism determined by positron emission tomography: a revisit. *J Cereb Blood Flow Metab* 1987;7:427–432.
17. Reivich M, Alavi A, Wolf A, et al. Glucose metabolic rate kinetic model parameter determinations in humans: the lumped constants and rate constants for [^{18}F]fluorodeoxy- and [^{11}C]deoxyglucose. *J Cereb Blood Flow Metab* 1985;5:179–192.
18. Cunningham VJ. The influence of transport and metabolism on brain glucose content. *Ann N Y Acad Sci* 1986;481:161–173.
19. Cremer JE, Cunningham VJ, Seville MP. Relationships between extraction and metabolism of glucose, blood flow, and tissue blood volume in regions of rat brain. *J Cereb Blood Flow Metab* 1983;3:291–302.
20. Hawkins RA, Mans AM, Davis DW, Hibbard LS, Lu DM. Glucose availability to individual cerebral structures is correlated to glucose metabolism. *J Neurochem* 1983;40:1013–1018.
21. Cornford EM, Hyman S, Swartz BE. The human brain GLUT1 glucose transporter: ultrastructural localization to the blood-brain barrier endothelia. *J Cereb Blood Flow Metab* 1994;14:106–112.
22. Lee W-H, Bondy CA. Ischemic injury induces brain glucose transporter gene expression. *Endocrinology* 1993;133:2540–2544.
23. Lawrence MS, Ho DY, Dash R, Sapolsky RM. Herpes simplex virus vectors overexpressing the glucose transporter gene protect against seizure-induced neuron loss. *Proc Natl Acad Sci* 1995;92:7247–7251.
24. Kuwabara H, Evans AC, Gjedde A. Michaelis-Menten constraints improved cerebral glucose metabolism and regional lumped constant measurements with [^{18}F]fluorodeoxyglucose. *J Cereb Blood Flow Metab* 1990;10:180–189.
25. Crane PD, Pardridge WM, Braun LD, Oldendorf WH. Kinetics of transport and phosphorylation of 2-fluoro-2-deoxy-D-glucose in rat brain. *J Neurochem* 1983;40: 160–167.
26. Pardridge WM, Crane PD, Mietus LJ, Oldendorf WH. Kinetics of regional blood-brain barrier transport and brain phosphorylation of glucose and 2-deoxyglucose on the barbiturate-anesthetised rat. *J Neurochem* 1982;38:560–568.
27. Crane PD, Pardridge WM, Braun LD, Nyerges AM, Oldendorf WH. The interaction of transport and metabolism on brain glucose utilization: a reevaluation of the lumped constant. *J Neurochem* 1981;36:1601–1604.
28. Sols A, Crane RK. Substrate specificity of brain hexokinase. *J Biol Chem* 1954;210: 581–595.
29. Pardridge WM, Oldendorf WH. Kinetics of blood-brain barrier transport of hexoses. *Biochim Biophys Acta* 1975;382:377–392.
30. Theodore WH, Gaillard WD, Sato S, Kufta C, Leiderman D. Positron emission tomographic measurement of cerebral blood flow and temporal lobectomy. *Ann Neurol* 1994;36:241–244.
31. Leiderman DB, Balsih M, Sato S, et al. Comparison of PET measurements of cerebral blood flow and glucose metabolism for the localization of human epilepstic foci. *Epilepsy Res* 1992;13:153–158.
32. Pawlik G, Fink GR, Weinhard K, Heiss W-D. Uncoupling of focal metabolism and hemodynamics in mesiolimbic temporal lobe epilepsy. *Epilepsia* 1993;34(suppl 2):186.
33. Gaillard WD, Fazilat S, White S, et al. Interictal metabolism and blood flow are uncoupled in temporal lobe cortex of patients with complex partial epilepsy. *Neurology* 1995;45:1841–1847.
34. Gjedde A. Calculation of cerebral glucose phosphorylation from brain uptake of glucose analogs in vivo: a re-examination. *Brain Res Brain Res Rev* 1982;4:237–274.
35. Gjedde A, Diemer NH. Autoradiographic determination of regional brain glucose content. *J Cereb Blood Flow Metab* 1983;3:303–310.